

# Dynamic analysis of planar mechanical systems with clearance joints using a new nonlinear contact force model<sup>†</sup>

Xupeng Wang, Geng Liu<sup>\*</sup> and Shangjun Ma

*School of Mechanical Engineering, Northwestern Polytechnical University, Xi'an Shanxi, 710072, China*

(Manuscript Received October 13, 2015; Revised November 23, 2015; Accepted November 26, 2015)

## Abstract

We investigated the dynamic behavior of planar mechanical systems with clearance joints. First, the contact effect in clearance joint was studied using a new nonlinear contact force model, and the rationality of this model was verified by the results of numerical simulations, which are based on a journal and bearing contact model. Then, the dynamic characteristics of a planar slider-crank mechanism with clearance were analyzed based on the new nonlinear contact force model, and the friction effect of clearance joint was also considered using modified Coulomb friction model. Finally, the numerical results of the influence of clearance size on the acceleration of slider are presented, and compared with the published experimental results. The numerical and experimental results show that the new nonlinear contact force model presented in this paper is an effective method to predict the dynamic behavior of planar mechanical system with clearance joints, and appears to be suitable for a wide range of impact situations, especially with low coefficient of restitution.

**Keywords:** Clearance joints; New nonlinear contact force model; Dynamic characteristics; Mechanical systems; Experimental results

## 1. Introduction

Mechanical systems usually consist of a number of components connected by kinematic joints, so called journal-bearing. With the demand for relative motion, and the errors of manufacturing and assembly, as well as the influence of wear, the clearance joints in mechanical systems are inevitable [1, 2]. Furthermore, clearance joints will have many effects on mechanical systems, such as vibration, wear and noise, which may reduce system reliability, kinematic accuracy and stability, even the life of mechanism. So modeling an accurate contact force model for dynamic simulation of mechanical systems with clearance joints is critical [3, 4].

Several different contact force models have been presented in the past to represent the contact effect of clearance joints [5]. As a pioneer study, Hertz presented the contact force with a nonlinear power function of indentation, which considers the influence of geometric and material characteristics between contact surfaces. Goldsmith [6] concluded that the Hertz model is more suitable when the contact material is hard and the initial velocity is low, and based on Hertz's works he proposed a modified contact force model. Liu et al. [7] proposed a new contact force model for cylindrical clearance joints based on the finite element analysis. However, all these con-

tact force models are purely elastic and do not consider the energy dissipation during the contact process. To overcome this drawback, based on Hertz's contact force model, several dissipative contact force models are shown by Hunt and Crossley [8], Lankarani and Nikravesh [9], Bai et al. [10], Wang and Liu [11]. The model proposed by Lankarani and Nikravesh [9] is most frequently used in dynamic simulation of multibody system with clearance joints.

A large number of researches have been done on the dynamic behavior of a multi-body system with clearance joints. Wand and Liu [12] studied the dynamic behavior of flapping-wing mechanism with clearance joint, and found that dynamic response of the flapping-wing mechanism exhibits a chaotic response. Xu and Li [13] studied the effects of clearance joints on the dynamic performance of a planar 2-DOF pick-and-place parallel manipulator using a contact force model considering hysteretic damping. Zhao and Bai [14] studied the dynamics analysis of space robot manipulator with joint clearance based on the software package of ADAMS. Flores [15] presented a methodology for dynamic modeling and analysis of multibody systems with clearance joints, and found that clearance size and operating conditions play a crucial role in predicting the dynamic responses of multibody systems. Flores [16] studied the wear in revolute clearance joints in multibody systems and investigated the wear process between contact bodies. Koshy et al. [17] studied the effect of contact force model on the dynamic response of mechanical systems, and

<sup>\*</sup>Corresponding author. Tel.: +86 29 88460411, Fax.: +86 29 88460411  
E-mail address: npuliug@nwpu.edu.cn

<sup>†</sup>Recommended by Associate Editor Eung-Soo Shin

© KSME & Springer 2016

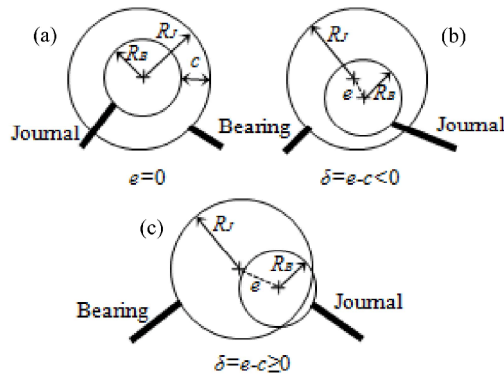


Fig. 1. Contact and separation of the journal relative to the bearing in a clearance revolute joint.

concluded that the selection of appropriate contact force model plays a crucial role in the dynamic response of mechanical systems. Yao et al. [18] presented an analytical model to describe the dynamic characteristics of a planar rotation beam with clearance joint. Zhao et al. [19] showed a parameter optimization method for planar joint clearance contact force model in order to improve the accuracy of dynamics response simulation for mechanism with joint clearance. Erkaya and Uzmay [20] investigated the kinematic and dynamic characteristics of a planar four-bar mechanism having joint clearance and link flexibility, and found that considering the effect of flexible link, values of peaks in flexible mechanism are less than those in rigid mechanism.

Our main goal was to conduct a study based on dynamic simulation of mechanical system with clearance joints. For this purpose, an accurate new nonlinear contact force model for revolute clearance joint is presented, then a large number of simulations are presented based on a simple journal-bearing joint and a typical slider-crank mechanism with clearance joint, and the numerical results also compared with the published experimental results.

## 2. Modeling revolute joint with clearance

In the general dynamic analysis of mechanical system with clearance joints, the revolute joints are considered as ideal or perfect, which means that two centers of journal and bearing coincide. However, the existence of clearance in joint is inevitable.

As shown in Fig. 1, there are three different relative motions between the journal and bearing: (i) Free flight mode, which means the centers of journal and bearing are coincident, or the eccentricity  $e$  is smaller than clearance  $c$ , and the journal and bearing are separated, (ii) impact mode, it appears at the end of the free flight mode when the  $e$  is equal to  $c$ , and (iii) continuous contact model; the contact is maintained and the  $e$  is bigger than  $c$ , as well as the normal and tangential contact forces. So it is important to effectively describe relative movement between the journal and bearing, as well as make an accurate judgment whether contacts occurs.

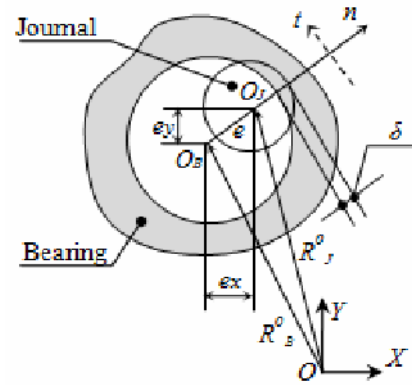


Fig. 2. Revolution joint clearance with contact.

Fig. 2 depicts a revolute clearance joint with contact in a mechanical system. The positional vectors of the bearing and journal are  $R_b^o$  and  $R_j^o$  in the globe inertia coordinate  $XOY$ , respectively. Point  $O_b$  and point  $O_j$  indicate the centers of bearing and journal. The clearance vector is given by [12, 15]

$$e = R_b^o - R_j^o, \quad (1)$$

where  $e$  represents the eccentricity vector of the centers between journal and bearing, which can be described as

$$e = \sqrt{e_x^2 + e_y^2}. \quad (2)$$

The relative deformation depth between journal and bearing can be defined by

$$\delta = e - (R_b - R_j). \quad (3)$$

The relative velocities in the normal and tangential directions between the surface of journal and bearing can be given by

$$\begin{cases} v_N = \delta' n \\ v_T = \delta' t \end{cases} \quad (4)$$

where  $n$  is the unit vector normal to the impact plane, and  $t$  represents the unit tangential vector, which can be obtained by reversing  $n$  for  $90^\circ$ .

## 3. Contact force modeling of joint with clearance

The best well-known impact force model is the Hertz's contact law, which can be expressed as

$$F = K \delta^n, \quad (5)$$

where  $K$  is the generalized stiffness parameter,  $n$  is the nonlinear power exponent, which is equal to 1.5 for metallic contact,

and  $\delta$  is the relative deformation depth. The stiffness coefficient  $K$  is given by [9]

$$K = \frac{4}{3\pi(\sigma_1 + \sigma_2)} \sqrt{\frac{R_B R_J}{R_B - R_J}}, \quad (6)$$

where  $R_B$  and  $R_J$  are the radius of bearing and journal, respectively, and the material parameter  $\sigma_i$  is given by

$$\sigma_i = \frac{1 - \nu_i^2}{\pi E_i}, (i = 1, 2), \quad (7)$$

where  $\nu_i$  and  $E_i$  are Poisson's ratio and Young's modulus associated with journal and bearing, respectively.

But the Hertz contact law is a purely elastic contact force model that does not account for the energy dissipation during the impact process [5, 11, 12]. Based on the Hertz contact force model, several dissipative contact force models are presented as follows.

Hunt and Crossley [8] represent a contact force model based on the pure elastic Hertz's law, and combined with a nonlinear viscoelastic element, which can be expressed as

$$F_N = K \delta^n \left[ 1 + \frac{3(1 - c_r)}{2} \frac{\delta}{\delta^{(+)}} \right], \quad (8)$$

where  $K$  is the contact stiffness parameter defined by Eqs. (6) and (7),  $c_r$  is the restitution coefficient, which may depend on initial impact velocity, geometry, and material properties, as well as contact time and friction.  $\delta^{(+)}$  is the initial impact velocity.

Based on the Hunt and Crossley work, a most popular and frequently used contact force model is defined by Lankarani and Nikravesh [9], which can be given by

$$F_N = K \delta^n \left[ 1 + \frac{3(1 - c_r^2)}{4} \frac{\delta}{\delta^{(+)}} \right]. \quad (9)$$

Bai et al. [10] present a new hybrid contact force model, which is based on the Lankarani-Nikravesh model and the improved Winkler elastic foundation model, and it can be defined by

$$F_N = K_n \delta^n + D_{\text{mod}} \delta'. \quad (10)$$

The nonlinear stiffness  $K_n$  can be defined as

$$K_n = \frac{1}{8} \pi E^* \sqrt{\frac{2\delta(3(R_B - R_J) + 2\delta)^2}{(R_B - R_J + \delta)^2}}, \quad (11)$$

where  $E^*$  is the composite modulus of the colliding bodies,

which can be expressed as

$$E^* = \left( \frac{1 - \nu_1^2}{E_1} + \frac{1 - \nu_2^2}{E_2} \right)^{-1} \quad (12)$$

where  $E_{1,2}$  and  $\nu_{1,2}$  are Young's modulus and Poisson's ratio associated with bearing and journal.

The damping coefficient is defined by

$$D_{\text{mod}} = \frac{3K_n(1 - c_r^2)e^{2(1 - c_r)}\delta^n}{4\delta^{(-)}}. \quad (13)$$

Based on the contact force model of Liu et al. [7] and contact force model of Lankarani and Nikravesh [9], Wang and Liu [11] introduced an improved contact force model for revolute joint with clearance in planar multi-body systems, which has a wider range of impact conditions to meet different clearance and load, and the model can be expressed as

$$F_N = \frac{\pi E^* L \delta^n}{2} \left( \frac{1}{2(c + \delta)} \right)^{1/2} + D_{\text{imp}} \delta', \quad (14)$$

where the first term represents the elastic forces, and the second term represents the energy dissipation, and clearance  $c = R_B - R_J$ ,  $R_B$  and  $R_J$  are the radii of bearing and journal illustrated in Fig. 1,  $D_{\text{imp}}$  is the improved damping coefficient and can be written as

$$D_{\text{imp}} = \text{Step}(\delta, 0, 0, \delta_{\text{max}}, D_{\text{max}}) = \begin{cases} 0 & \delta \leq 0 \\ D_{\text{max}} \left( \frac{\delta}{\delta_{\text{max}}} \right)^2 (3 - 2 \times \frac{\delta}{\delta_{\text{max}}}) & 0 < \delta < \delta_{\text{max}} \\ D_{\text{max}} & \delta_{\text{max}} \leq \delta \end{cases} \quad (15)$$

The  $D_{\text{max}}$  can be expressed as [11]

$$D_{\text{max}} = K_N(1 - c_r) / 680, \quad (16)$$

where  $K_N$  is the contact stiffness, which can be defined as

$$K_N = \frac{\pi E^* L \delta^n}{2} \left( \frac{n}{\delta} \left( \frac{1}{2(c + \delta)} \right)^{1/2} + \left( \frac{1}{2(c + \delta)} \right)^{-1/2} \right). \quad (17)$$

The models of Hunt and Crossley [8], and Lankarani and Nikravesh [9] are all appropriate for contact cases in which the coefficient of restitution is high, so the model presented by Wang and Liu [11] is also more accurate when the coefficient of restitution near to 1. To overcome this drawback, based on the work of Wang and Liu [11], this paper sets up an improved nonlinear contact force model as follows.

First, based on the elastic force of the Eq. (14), assuming an improved nonlinear stiffness coefficient exists, which can

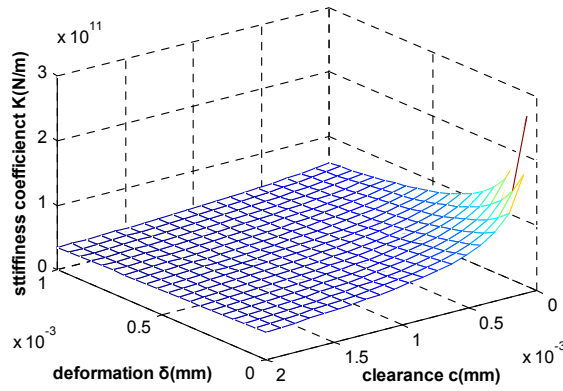


Fig. 3. Nonlinear coefficient of contact stiffness varying with clearance and deformation.

satisfy Eq. (18) as follows:

$$F_N' = \frac{\pi E^* L \delta^n}{2} \left( \frac{1}{2(c + \delta)} \right)^{1/2} = K_i \delta^n. \quad (18)$$

So the nonlinear stiffness coefficient  $K_i$  can be defined as Eq. (19), and the varying of stiffness with clearance and deformation can be illustrated by Fig. 3.

$$K_i = \frac{\pi E^* L}{2} \left( \frac{1}{2(c + \delta)} \right)^{1/2}. \quad (19)$$

Then the improved damping coefficient can also be given by

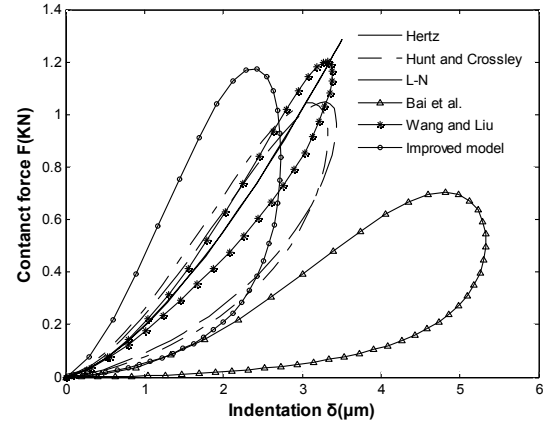
$$D_i = \frac{3(1 - c_r^2) e^{2(1 - c_r)} \delta^n}{4 \delta^{(-)}} K_i. \quad (20)$$

Finally, the improved nonlinear contact force model can be defined as

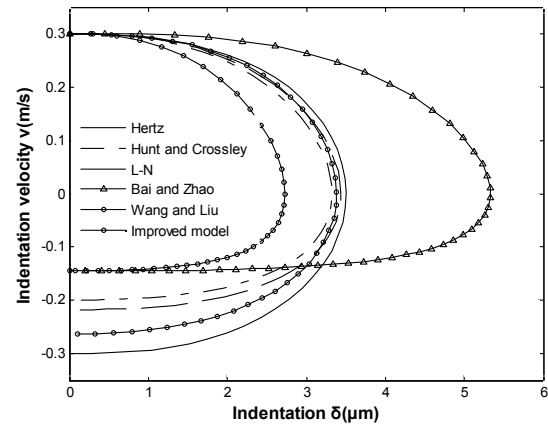
$$F_{Ni} = K_i \delta^n + D_i \delta' \\ = \frac{\pi E^* L \delta^n}{2} \left( \frac{1}{2(c + \delta)} \right)^{1/2} \left( 1 + \frac{3(1 - c_r^2) e^{2(1 - c_r)} \delta'}{4 \delta^{(-)}} \right). \quad (21)$$

To verify the rationale of the improved nonlinear contact force model, a typical contact model of bearing and journal in revolute clearance joint is presented. The contact force, indentation and velocity of bearing and journal in revolute clearance joint are analyzed by using the different contact force models. The radii of bearing and journal are 10 mm and 9.9 mm, respectively. The length of bearing is 15 mm. The mass of journal is 0.04 kg, the initial velocity of journal is 0.3 m/s and the bearing is fixed. The bearing and journal have the same Young's modulus of 207 GPa, as well as Poisson's ratio of 0.3.

Fig. 4 shows the force-indentation and the velocity-indentation diagrams for the bearing and journal presented above, which are based on different contact force models with



(a)



(b)

Fig. 4. Externally colliding spheres modeled by new model, Hertz, Lee and Wang, Lankarani and Nikravesh, Gonthier et al., Flores et al. contact force models: (a) Force-indentation relation; (b) velocity-indentation relation.

the coefficient of restitution of 0.5. It can be found that the contact processes are different with the different contact force models. As illustrated by Fig. 4(a) the contact responses based on Hunt and Crossley model, L-N model, Wang and Liu model and improved nonlinear contact force model are similar, but the maximum contact force based on improved model as well as Wang and Liu model [11] are more close to Hertz's model than others'. Concerning the model of Bai et al., for the same initial coefficient, it has smaller contact force but larger indentation than other models, so that the Bai et al. model underestimates the contact stiffness and, as a result, the contact forces. However, the contact stiffness is critical in simulations and should be selected properly, because it may affect the dynamic behavior significantly [21]. From Fig. 4(b) it can be concluded that compared to the Hertz model, Hunt and Crossley model [8], Lankarani and Nikravesh model [9], and Wang and Liu model [11], the departing velocity based on Bai et al. [10] model and improved nonlinear contact force model are more nearly 0.15 m/s, which is consistent with the coefficient of restitution.

Table 1. Simulation results with fixed  $c_r$ ,  $\delta'(-)$  and varied  $c$ .

Name	$c$	0.01	0.1	0.5	1
$M_{\text{Imp}}$	$\delta^{(+)}(\text{m/s})$	0.1448	0.1448	0.1448	0.1448
	$c_r$	0.4827	0.4827	0.4827	0.4827
	Error	3.46%	3.46%	3.46%	3.46%
$M_{\text{L-N}}$	$\delta^{(+)}(\text{m/s})$	0.2176	0.2176	0.2176	0.2176
	$c_r$	0.7253	0.7253	0.7253	0.7253
	error	45.06%	45.06%	45.06%	45.06%

Table 2. Simulation results with fixed  $c$ ,  $\delta^{(-)}$  and varied  $c_r$ .

Name	$c_r$	0.3	0.5	0.9	1
$M_{\text{Imp}}$	$\delta^{(+)}(\text{m/s})$	0.098	0.1448	0.2687	0.3
	$c_r$	0.3267	0.4827	0.8957	1
	Error	8.889%	3.467%	0.482%	0
$M_{\text{L-N}}$	$\delta^{(+)}(\text{m/s})$	0.2053	0.2176	0.274	0.3
	$c_r$	0.6843	0.7253	0.9133	1
	Error	128.1%	45.06%	1.48%	0

Additionally, the actual restitution coefficient  $c_r$  is related to Newton's impact hypothesis and can be defined by Eq. (22):

$$c_r' = -\frac{\delta^{(+)}}{\delta^{(-)}} \quad 0 \leq c_r' \leq 1, \quad (22)$$

where  $\delta^{(+)}$  represents the velocity after impact. The relative error of contact force modal is also given by Eq. (23)

$$\text{error} = \left| \frac{c_r' - c_r}{c_r} \right| \times 100\%. \quad (23)$$

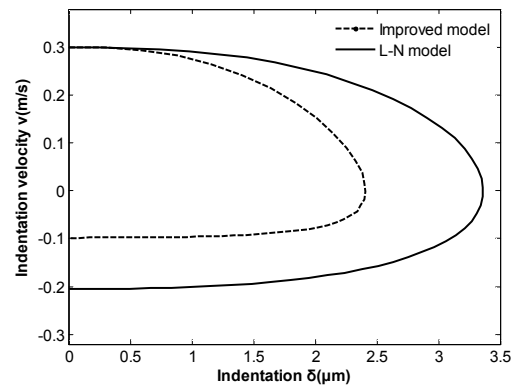
The simulations with contact model are presented under different clearance size  $c$ , restitution coefficient  $c_r$  as well as initial velocity  $\delta^{(-)}$ , which are based on improved nonlinear contact force model and the most frequently used Lankarani and Nikravesh model.

Table 1 shows the results with restitution coefficient  $c_r$  of 0.5, initial velocity  $\delta^{(-)}$  0.3 m/s, and clearance size  $c$  is varied from 0.01 mm to 1 mm. It can be concluded that if the restitution coefficient  $c_r$  and initial velocity  $\delta^{(-)}$  are fixed, the relative error of contact force modals is not changed although the clearance size  $c$  is varied, but the value based on improved nonlinear contact force model is only 3.46%, which is obviously smaller than Lankarani and Nikravesh model's 45.06%.

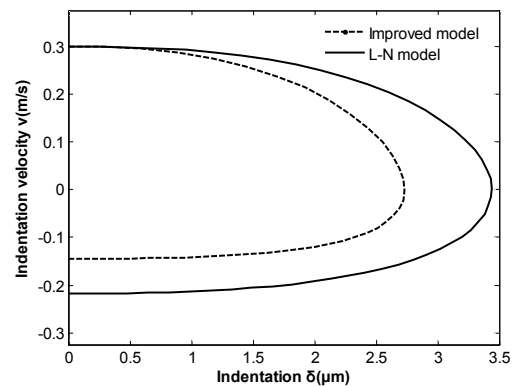
Table 2 presents the results for the case of the clearance size  $c$  of 0.1 mm, initial velocity  $\delta^{(-)}$  0.3 m/s, but the restitution coefficient  $c_r$  is varied from 0.3 to 1. Table 2 shows that with the fixed clearance size and initial velocity  $\delta^{(-)}$ , the relative error of contact force modals is gradually decreased when restitution coefficient  $c_r$  is increased. However, the relative error of the improved nonlinear contact force model is also far smaller than Lankarani and Nikravesh model's, especially

Table 3. Simulation results with fixed  $c$ ,  $c_r$  and varied  $\delta^{(-)}$ .

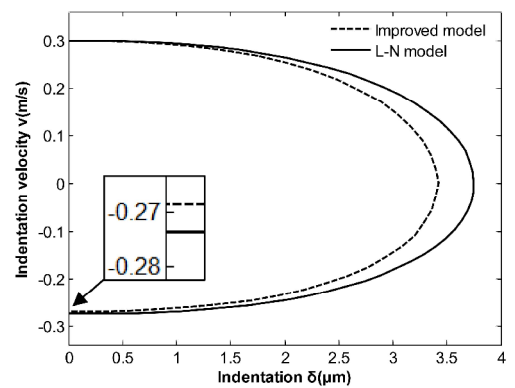
Name	$\delta^{(-)}$	$\delta'(-)$	$3\delta^{(-)}$	$5\delta^{(-)}$	$10\delta^{(-)}$
$M_{\text{Imp}}$	$\delta^{(+)}(\text{m/s})$	0.1448	0.4343	0.7239	1.4478
	$c_r$	0.4827	0.4826	0.4826	0.4826
	Error	3.46%	3.48%	3.48%	3.48%
$M_{\text{L-N}}$	$\delta^{(+)}(\text{m/s})$	0.2176	0.6527	1.0879	2.1757
	$c_r$	0.7253	0.7252	0.7253	0.7252
	Error	45.06%	45.04%	45.06%	45.04%



(a)



(b)



(c)

Fig. 5. Velocity-indentation curves with improved model and Lankarani and Nikravesh models: (a)  $c_r = 0.3$ ; (b)  $c_r = 0.5$ ; (c)  $c_r = 0.9$ .

when the restitution coefficient  $c_r$  is small, which also can be clearly illustrated by the Fig. 5.

Table 3 illustrates the outcomes when the clearance size  $c$  is 0.1 mm, the restitution coefficient  $c_r$  is 0.5, and the initial velocity  $\delta^{(c)}$  is varied from  $\delta^{(c)}$  (0.3 m/s) to  $10\delta^{(c)}$  (3 m/s), which is similar to the results of Table 1.

The comparison of the numerical simulations presented above proves that the improved nonlinear contact force model has better calculation precision for lower and higher coefficient of clearance size, restitution coefficient and initial velocity.

A modified Coulomb friction force model is used to depict the friction effect in clearance joint, which can be expressed as [22]

$$F_T = -c_f c_d F_N \operatorname{sgn}(V_T), \quad (24)$$

where  $c_f$  is the friction coefficient,  $F_N$  is the normal force, and  $V_T$  is the relative tangential velocity, the dynamic correction coefficient  $c_d$ , which can prevent the friction force changes direction for almost null values of the tangential velocity, is defined by

$$c_d = \begin{cases} 0 & \text{if } |V_T| \leq v_0 \\ \frac{|V_T| - v_0}{v_1 - v_0} & \text{if } v_0 < |V_T| < v_1 \\ 1 & \text{if } |V_T| \geq v_1 \end{cases} \quad (25)$$

where  $v_0$  and  $v_1$  are given tolerances for the tangential velocity [22].

#### 4. Application case: Slider-crank mechanism

To further validate the improved contact force model and investigate the effect of clearance size on dynamic characteristics of mechanical systems with clearance joints, a planar slider-crank mechanism [23] with clearance joint between the connecting rod and slider is used as numerical example. Fig. 6 shows the configuration of the mechanism with one clearance revolute joint between connecting rod and slider. For comparing with the experimental results presented by Flores et al. [23], the same parameters of slider-crank mechanism with those defined in Ref. [23] are adopted in this paper. The diameter of bearing is 22.25 mm, the length of bearing is 15 mm, and clearance sizes are equal to 0.1 mm, 0.25 mm, 0.5 mm and 1 mm, respectively. Note that based on the ISO system information [24, 25], the suitable clearance sizes of this bearing are in the range of 0.022 mm to 0.325 mm. The mass and inertia properties of the slider-crank mechanism are shown in Table 4. And the coefficient of restitution is 0.46, coefficient of friction is 0.01, Young's modulus is 207 GPa and Poisson's ratio is 0.3. Define that the slider-crank mechanism is initialized with a crank speed of 200 rpm, and assume that the speed is constant during the simulation. Then the numerical simula-

Table 4. Mass and inertia properties of slider-crank mechanism.

Body	Length [m]	Mass [kg]	Moment of inertial [kgm <sup>2</sup> ]
Crank	0.05	17.900	0.460327
Connecting rod	0.30	1.130	0.015300
Slider	-	1.013	0.000772

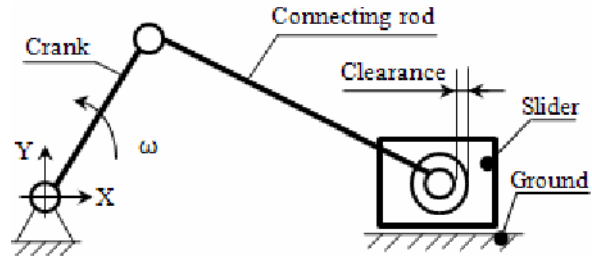


Fig. 6. Slider-crank mechanism with a revolute clearance.

tions are conducted by using Matlab Simulink, with variable-step Runge-Kutta integrator scheme. In the simulations, the integration step size is 1e-6s, and integration tolerance is 1e-7.

Numerical results of slider acceleration response with different clearance sizes are presented in Figs. 7(a), 8(a), 9(a) and 10(a), which are compared with the numerical results for slider-crank mechanism with perfect joint. The corresponding experimental results presented by Flores et al. [23] are shown in Figs. 7(b), 8(b), 9(b) and 10(b), and the experimental results are also compared with the numerical results for slider-crank mechanism with perfect joint. Comparing the numerical and experimental results with same clearance size, shown in Figs. 7(a), 8(a), 9(a) and 10(a), very similar dynamic behaviors of slider acceleration are obtained: (i) With the effect of clearance joint, the slider acceleration curves are obviously shaky around the ideal value, (ii) when clearance sizes change from 0.1 mm, 0.25 mm, 0.5 mm to 1 mm, the vibration becomes serious, and the vibration amplitude also becomes larger, and (iii) with the increase of clearance size, the vibration frequency tends to be lower. All those dynamic behaviors also can be drawn by experimental results in Figs. 7(b), 8(b), 9(b) and 10(b), although the maximum vibration amplitude in simulation is smaller than that from experiment with same clearance size. So it can be concluded that the influence law and influence numerical magnitude on slider acceleration response are similar to numerical and experimental results.

The differences between numerical and experimental results presented in Figs. 7-10 may be caused by factors as follows: (i) The clearance size is assumed to be equal and without change during simulation, which is different from actual, (ii) the selection of suitable restitution and friction coefficients, because small variations on these parameters can significantly change the system response, (iii) the flexibility of links, and lubrication action and the plastic deformation in the clearance joint are neglected in the numerical simulations, which may



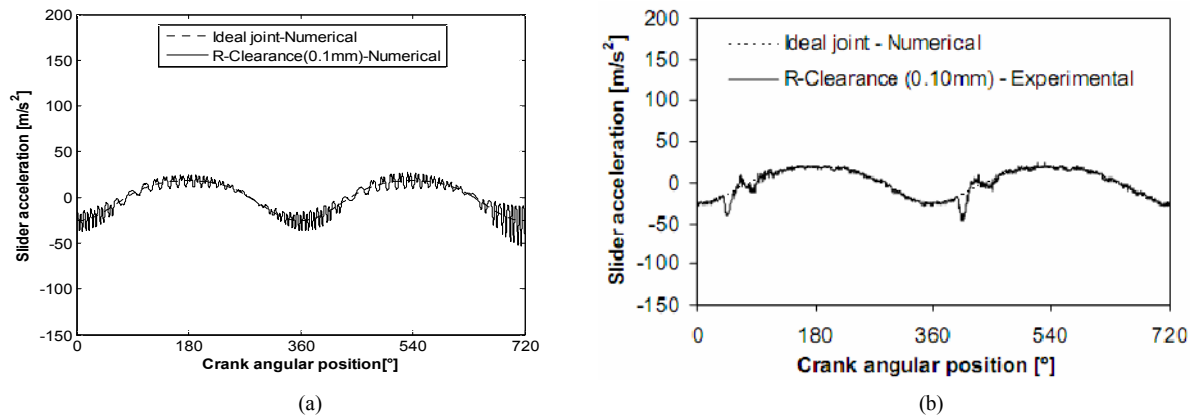


Fig. 7. Slider accelerations with clearance size  $c = 0.1$  mm from (a) simulation; (b) experiment [23].

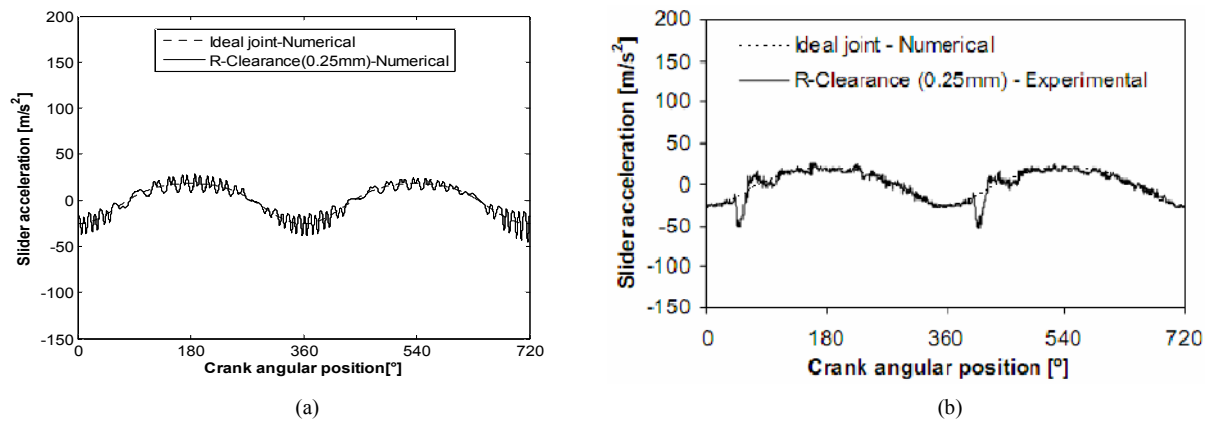


Fig. 8. Slider accelerations with clearance size  $c = 0.25$  mm from (a) simulation; (b) experiment [23].

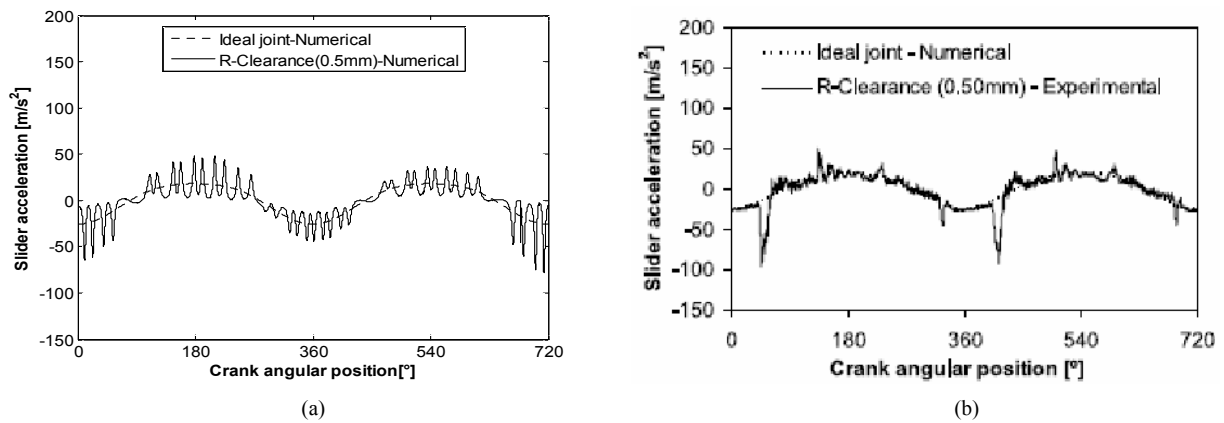


Fig. 9. Slider accelerations with clearance size  $c = 0.5$  mm from (a) simulation; (b) experiment [23].

have serious effect on the dynamic response of mechanism, and (iv) in the experiment, the clearances of ground-crank, crank-connecting rod and ground-slider exist and the values are 0.009 mm, 0.005 mm and 0.001 mm, respectively, but all these clearances are ignored and considered to be ideal in numerical simulation, which may also have an influence on numerical results.

## 5. Conclusion

To make an accurate analysis of the dynamic characteristics of mechanical systems with clearance joints, a new nonlinear contact force model for cylindrical clearance joint was presented, which is a combination of a nonlinear contact law with nonlinear contact stiffness, and accounts for the axial dimen-

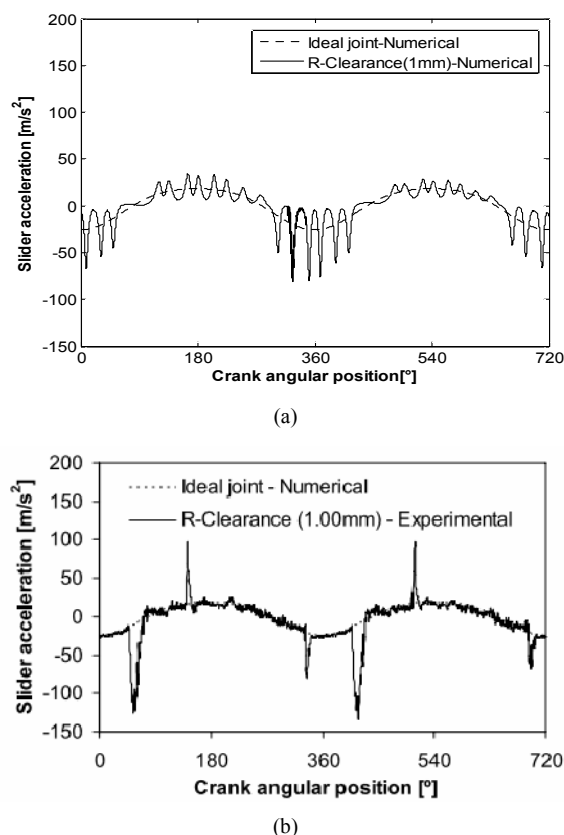


Fig. 10. Slider accelerations with clearance size  $c = 1$  mm from (a) simulation; (b) experiment [23].

sion of bearing. The friction effect is also measured by a modified Coulomb friction. Then a large number of dynamic simulations were presented based on a typical contact model of bearing and journal, and a planar slider-crank mechanism with clearance joint between connecting rod and slider. By comparing the numerical results with different contact force models and the results of experimental, the new nonlinear contact force model can effectively describe contact force of joints for lower and higher coefficient of clearance size, restitution coefficient and initial velocity. And the dynamic response of slider acceleration, which is based on the new nonlinear contact force model, is similar to the experimental results published, which provides a new method to predict the dynamic behavior of planar mechanical system with clearance joints.

Note that the results presented do not consider the flexibility of links, lubrication action and the plastic deformation in the clearance joint, which also have obvious influence on the behaviors of the mechanical systems and should be considered in future researches.

### Acknowledgment

This work is supported by the Education Research Foundation for the Doctoral Program of Ministry (20126102110019),

The 111 Project (Grant No. B13044), National Natural Science Foundation of China (Grant No. 51505381 and 51275423) and Fundamental Research Funds for the Central Universities (Grant No. 3102015JCS05008), China. The authors would like to express their appreciation to the agencies.

### References

- [1] S. Erkaya and I. Uzmay, Modeling and simulation of joint clearance effects on mechanisms having rigid and flexible links, *JMST*, 28 (8) (2014) 2979-2986.
- [2] P. Flores and J. Ambrósio, Revolute joints with clearance in multibody systems, *Computers and Structures*, 82 (2004) 1359-1369.
- [3] Q. Tian, Y. Zhang, L. Chen and P. Flores, Dynamics of spatial flexible multibody systems with clearance and lubricated spherical joints, *Computers and Structures*, 87 (2009) 913-929.
- [4] T. K. Naskar and S. Acharyya, Measuring cam-follower performance, *Mechanism and Machine Theory*, 45 (2010) 678-691.
- [5] M. Machado, P. Moreira, P. Flores and H. M. Lankarani, Compliant contact force models in multibody dynamics: Evolution of the Hertz contact theory, *Mechanism and Machine Theory*, 53 (2012) 99-121.
- [6] W. Goldsmith, *Impact-the theory and physical behaviour of colliding solids*, Edward Arnold Ltd., London, England (1960).
- [7] C. S. Liu, K. Zhang and L. Yang, The FEM analysis and approximate model for cylindrical joints with clearances, *Mechanism and Machine Theory*, 42 (2007) 183-197.
- [8] K. H. Hunt and F. R. E. Crossley, Coefficient of restitution interpreted as damping in vibroimpact, *J. of Applied Mechanics*, 7 (1975) 440-445.
- [9] H. M. Lankarani and P. E. Nikravesh, A contact force model with hysteresis damping for impact analysis of multi-body systems, *J. of Mechanical Design*, 112 (1990) 368-376.
- [10] Z. F. Bai and Y. Zhao, A hybrid contact force model of revolute joint with clearance for planar mechanical systems, *International J. of Non-Linear Mechanics*, 48 (2013) 15-36.
- [11] X. P. Wang and G. Liu, Modeling and simulation of revolute joint with clearance in planar multi-body systems, *JMST*, 29 (10) (2015) 4113-4120.
- [12] X. P. Wang and G. Liu, Nonlinear behavior analysis of a flapping-wing mechanism with clearance joint, *Applied Mechanics and Materials*, 743 (2015) 107-114.
- [13] L. X. Xu and Y. G. Li, Investigation of clearance joints on the dynamic performance of a planar 2-DOF pick-and-place parallel manipulator, *Robotics and Computer-Integrated Manufacturing*, 30 (2014) 62-73.
- [14] Y. Zhao and Z. F. Bai, Dynamics analysis of space robot manipulator with joint clearance, *Acta Astronautica*, 68 (2010) 1147-1155.
- [15] P. Flores, A parametric study on the dynamic response of planar multibody systems with multiple clearance joints,



*Nonlinear Dynamics*, 61 (2010) 633–653.

- [16] P. Flores, Modeling and simulation of wear in revolute clearance joints in multibody systems, *Mechanism and Machine Theory*, 44 (2009) 1211–1222.
- [17] C. S. Koshy, P. Flores and H. M. Lankarani, Study of the effect of contact force model on the dynamic response of mechanical systems with dry clearance joints: Computational and experimental approaches, *Nonlinear Dynamics*, 73 (2013) 325–338.
- [18] X. G. Yao et al., Dynamic analysis for planar beam with clearance joint, *J. of Sound and Vibration*, 03/2015; 339. DOI: 10.1016/j.jsv.2014.11.001.
- [19] H. Y. Zhao et al., A parameters optimization method for planar joint clearance model and its application for dynamics simulation of reciprocating compressor, *J. of Sound and Vibration*, 05/2015, 344, DOI: 10.1016/j.jsv.2015.01.044.
- [20] S. Erkaya, Prediction of vibration characteristics of a planar mechanism having imperfect joints using neural network, *JMST*, 26 (5) (2012) 1419–1430.
- [21] J. S.-S. Wu et al., The effect of bending loads on the dynamic behaviors of a rolling guide, *JMST*, 26 (3) (2012) 671–680.
- [22] J. A. C. Ambrósio, Impact of rigid and flexible multibody systems: Deformation Description and Contact Models, *Virtual Nonlinear Multibody Systems*, 2 (2002) 15–33.
- [23] P. Flores et al., Numerical and experimental investigation on Multibody systems with revolute clearance joints, *Nonlinear Dynamics*, 65 (4) (2011) 383–398.
- [24] BS EN ISO 286-1:2010, *Geometrical Product Specifications (GPS)-ISO code system for tolerance on linear sizes, Part 1: Basis of tolerances, deviations and fits* (2010).
- [25] BS EN ISO 286-2:2010, *Geometrical Product Specifications (GPS)-ISO code system for tolerance on linear sizes, Part 2: Tables of standard tolerance classes and limit deviations for holes and shafts* (2010).

*tions for holes and shafts* (2010).



prototype design and impact dynamics of planar mechanism with clearance joints.



cal dynamic design, mechanical systems dynamics, simulation and virtual prototype design, tribology, contact mechanics and numerical methods.



**Xupeng Wang** is a Ph.D. candidate at Northwestern Polytechnical University in Xi'an, China. He received his M.S. from Xi'an University of Technology. He is a senior engineer in the field of mechanical design and dynamic simulations. His research interests include CAD/CAE, multibody dynamics, virtual

**Geng Liu** is a professor and supervisor of Ph.D. students and director of the institute for Engineering Design and Simulation at Northwestern Polytechnical University (NWPU) in Xi'an, China. He received his M.S. in NWPU and Ph.D. from Xi'an Jiao tong University. His research interests include mechani-

**Shangjun Ma** is an assistant researcher at Northwestern Polytechnical University (NWPU) in Xi'an, China. He received his M.S. and Ph.D. from NWPU. His research interests include electromechanical actuator (EMA) and planetary roller screw mechanism (PRSM).